Dalton Transactions

Accepted Manuscript

This article can be cited before page numbers have been issued, to do this please use: T. Okamura, R. Furuya and K. Onitsuka, *Dalton Trans.*, 2015, DOI: 10.1039/C5DT00053J.

This is an *Accepted Manuscript*, which has been through the Royal Society of Chemistry peer review process and has been accepted for publication.

Accepted Manuscripts are published online shortly after acceptance, before technical editing, formatting and proof reading. Using this free service, authors can make their results available to the community, in citable form, before we publish the edited article. We will replace this *Accepted Manuscript* with the edited and formatted *Advance Article* as soon as it is available.

You can find more information about *Accepted Manuscripts* in the Information for Authors.

Please note that technical editing may introduce minor changes to the text and/or graphics, which may alter content. The journal's standard Terms & Conditions and the Ethical guidelines still apply. In no event shall the Royal Society of Chemistry be held responsible for any errors or omissions in this *Accepted Manuscript* or any consequences arising from the use of any information it contains.

ROYAL SOCIETY OF CHEMISTRY

www.rsc.org/dalton

View Article Online
DOI: 10.1039/C5DT00053J

Journal Name

RSCPublishing

ARTICLE

Cite this: DOI: 10.1039/x0xx00000x

Synthesis and structures of soluble magnesium and zinc carboxylates containing intramolecular NH•••O hydrogen bonds in nonpolar solvents†

Taka-aki Okamura,* Ryosuke Furuya and Kiyotaka Onitsuka

Received 00th January 2012,
Accepted 00th January 2012

DOI: 10.1039/x0xx00000x

www.rsc.org/

Readily soluble magnesium and zinc carboxylates [M(**Ln**)$_2$(H$_2$O)$_4$] (**MLn$_2$**) (M = Mg, Zn; **L1** = O$_2$C-2-Ar$_3$CCONH-6-*n*-BuCONHC$_6$H$_3$; **L2** = O$_2$C-2-Ar$_3$CCONHC$_6$H$_4$; Ar = 4-*t*-BuC$_6$H$_4$) containing intramolecular NH···O hydrogen bonds in nonpolar solvents were synthesized and their molecular structures were determined by X-ray analysis. The complexes were crystallized in the *trans* or *cis* configuration. The M–O bond distances were dependent on the mode of the hydrogen bonds. ^{1}H NMR spectral measurements revealed a fast *trans*-*cis* isomerization of **MLn$_2$** in CDCl$_3$, which was converted into a unique *fac*-[M(**Ln**)$_3$(H$_2$O)$_3$]$^-$ (*fac*-[**MLn$_3$**]$^-$) by the addition of equimolar [**Ln**]$^-$. The theoretical calculations supported the existence of the facial configuration. The coordinated water molecules of **MLn$_2$** were detected by ^{1}H NMR spectroscopy and the acidity was estimated in the order of **ML1$_2$** > **ML2$_2$**. Calcium afforded only dinuclear complex, [Ca$_2$(**L1**)$_2$(H$_2$O)$_5$(1,4-dioxane)] (**Ca$_2$L1$_4$**), which showed low hydrolytic activity.

Introduction

Naturally abundant magnesium is essential in biological processes involving phosphorylated compounds, such as repair, duplication, expression, and storage of genetic information, and energy metabolism processes.[1-4] These are closely associated with the life cycle of viruses and serious diseases.[5-7] Magnesium-dependent phosphatase is a prevalent enzyme that requires Mg^{2+} ions or analogous divalent metal ions (normally Mn^{2+}) in order to function.[2] The active sites are usually octahedral six-coordinated complexes containing labile Mg–O (carboxylate) bonds, which are supported by high intracellular a concentration of Mg^{2+} ions *in vivo*.[8,9]

In spite of the importance of the chemistry of magnesium carboxylates, reports regarding their solution structures are very limited.[10] Theoretical approaches using crystal structures of enzymes or synthetic models have given us some insights into their solution structures and the mechanisms of their hydrolytic reactions involving inner-sphere/outer-sphere pathways.[11–17] Many magnesium carboxylates have been reported and structurally characterized.[15,18] However, most of these are sparingly soluble in nonpolar solvents and dissociate to solvated ion pairs in a polar solution.[19,20] At the metal-binding site of ribonucleases, three carboxylates are conserved. Two of the three carboxylates are bound moderately to a metal ion. Theoretical predictions have indicated that the Mg^{2+} ion interacts with the third carboxylate in the outer shell of the protein matrix while the biologically inactive Ca^{2+} ion prefers to bind the third carboxylate in a chelate fashion.[21,22] Moreover, a hydrated Mg^{2+} ion can thermodynamically accept up to the third carboxylate in a medium with a low dielectric constant ($\varepsilon \leq 4$).[12]

Recently, we reported the significant contributions of intramolecular NH···O hydrogen bonds to Mg–O bonds in magnesium carboxylate complexes, as evidenced by X-ray analysis and theoretical calculations. The direct hydrogen bond to the coordinated oxygen atom of the carboxy group elongates the Mg–O (carboxylate) bond and shortens the Mg–OH$_2$ bonds, while the hydrogen bond to the uncoordinated carboxy oxygen atom shortens the Mg–O (carboxylate) bond. The opposite effect was also seen, depending on the mode of the hydrogen bond, which led to the proposal of a new switching mechanism based on controlling the acidity of the coordinated water molecule by regulating the strength of the Mg–OH$_2$ bond.[23] However, the insolubility of the complexes prevented an investigation of the real solution structures and experimental evaluation of the hydrolytic activity.

In a study on molybdenum enzyme models, we found that the very bulky and hydrophobic Ar$_3$CCONH (Ar = 4-*t*-BuC$_6$H$_4$) group sufficiently covered the ionic core of monooxomolybdenum dithiolate, and surprisingly, improved the solubility in nonpolar solvents.[24,25] Such low-dielectric media simulate the buried metal-binding cavity in the native protein matrix.[26] This finding encouraged us to apply these groups to magnesium carboxylates with ionic bonds.

View Article Online
DOI: 10.1039/C5DT00053J
Journal Name

In this Article, we present the synthesis of readily soluble carboxylic acids with the Ar_3CCONH groups, 2,6-$(Ar_3CCONH)_2C_6H_3COOH$ (**L0**H), 2-Ar_3CCONH-6-*n*-$BuCONHC_6H_3COOH$ (**L1**H), and 2-$Ar_3CCONHC_6H_4COOH$ (**L2**H). Sterically hindered **L0**H was designed to prevent the second coordination of the ligand to give $[Mg(\mathbf{L0})(H_2O)_5]^+$, with water coordinated *trans* to the carboxylate ligand, which is analogous to the crystal structure of $[Mg(O_2C\text{-}2\text{-}CH_3CONHC_6H_4)(H_2O)_5]^+$.[23] However, this trial met with failure. The desired magnesium complexes with **L1** or **L2** were readily soluble in nonpolar solvents. The corresponding zinc complexes with a stronger Zn–O bond[26] were synthesized for comparison. The analogous complexes of the biologically inactive Ca^{2+} ion were also prepared. The molecular structures of $\mathbf{MLn_2}$ in the crystal and the hydrolytic reactions have already been communicated.[27] A detailed description is presented here with additional data; moreover, the behavior of the complexes in solution and the formation of novel anionic tris(carboxylate) complexes are discussed. Hydrolysis of phosphoric ester by the metal carboxylates is also mentioned.

Experimental

All solvents were dried and distilled before use and amidation was carried out under argon atmosphere using Schlenk technique. Ar_3CCOCl (Ar- = *t*-BuC_6H_4-) and 2,6-$(CH_3CONH)_2C_6H_3COOH$ were prepared by the literature procedure.[25,28]

2,6-$(Ar_3CCONH)_2C_6H_3COOH$ (L0H)

2,6-$(CH_3CONH)_2C_6H_3COOH$ (0.170 g, 0.72 mmol) was suspended in a 10% HCl aqueous solution (20 mL). After stirring for 30 min at 90 °C, the suspension changed to a pale yellow solution. The aqueous solution which contains 2,6-$(NH_2)_2C_6H_3COOH{\cdot}2HCl$ was basified with $NaHCO_3$, and the solution was washed with Et_2O and dried under reduced pressure. To the suspension of the residue in CH_2Cl_2 (30 mL) was added triethylamine (0.50 mL, 3.6 mmol), the mixture was cooled in an ice bath, and the color of the mixture turned yellow. The solution of Ar_3CCOCl (0.683 g, 1.4 mmol) in CH_2Cl_2 (10 mL) was added carefully to the mixture cooling in an ice bath. After stirring overnight at 0 °C, the mixture was dried under reduced pressure, and the residue was extracted with dichloromethane. The organic layer was washed with 2% HCl aq, water, 4% $NaHCO_3$ aq, water, and sat. NaCl aq., successively. The organic layer was dried over Na_2SO_4 and evaporated to dryness. The residue was recrystallized from ethyl acetate to give colorless crystals. Yield: 0.452 g (61%). ^{1}H NMR (500 MHz, $CDCl_3$): δ7.32 (d, 12H, Ar), 7.25 (d, 12H, Ar), 1.31 (s, 27H, *t*-Bu). Anal. Calcd for $C_{75}H_{92}N_2O_6$ ((2,6-$Ar_3CCONH)_2C_6H_3COOH){\cdot}AcOEt$): C, 80.61; H, 8.31; N, 2.51. Found: C, 80.41; H, 8.21; N, 2.60.

2-Ar_3CCONH-6-*n*-$BuCONHC_6H_3COOH$ (L1H)

2,6-$(CH_3CONH)_2C_6H_3COOH$ (1.02 g, 4.3 mmol) was suspended in a 10% HCl aqueous solution (144 mL). After stirring for 30 min at 90 °C, the suspension changed to a pale yellow solution. The resulting aqueous solution of 2,6-$(NH_2)_2C_6H_3COOH{\cdot}2HCl$ was basified with $NaHCO_3$, washed with Et_2O, and dried under reduced pressure. The residue was suspended in CH_2Cl_2 (20 mL). Upon the addition of triethylamine (3.5 mL, 25 mmol) cooling in an ice bath, the mixture turned yellow. A solution of Ar_3CCOCl (2.02 g, 4.4 mmol) in CH_2Cl_2 (15 mL) was added carefully to the mixture cooling in an ice bath. After stirring overnight at 0 °C, the mixture was concentrated to dryness under reduced pressure. Toluene was added to the residue and was washed with 2% HCl aq. and sat. NaCl aq., successively. The solution was dried over $MgSO_4$ and evaporated to dryness under reduced pressure. The residue was recrystallized from ethanol to give colorless crystals, which were removed by filtration, and the filtrate was evaporated. The residue (1.45 g, 2.5 mmol) and NEt_3 (1.8 mL, 12 mmol) were dissolved in CH_2Cl_2 (20 mL) cooling in dryice/methanol bath and then valeryl chloride (0.26 mL, 2.2 mmol) in CH_2Cl_2 (20 mL) was added dropwise to the solution. The resulting yellow solution was stirred cooling in dryice/methanol bath for 6.5 h and at 2 °C for 19 h. The solution was concentrated to dryness under reduced pressure. Toluene was added to the residue and washed with 2% HCl aq. and sat. NaCl aq., successively. The solution was dried over Na_2SO_4 and evaporated. The residue was recrystallized from ethanol to give colorless crystalline solid and yellow solution. Yellow solution was separated and concentrated under reduced pressure. Addition of *n*-hexane to the residue gave colorless crystalline solid. Yield: 469 mg (16%). ^{1}H NMR (500 MHz, $CDCl_3$): δ9.94(s, 1H, NH), 9.38(s, 1H, NH), 8.23 (m, 2H, Ar), 7.49 (d, 1H, Ar), 7.30 (d, 6H, Ar), 7.19 (d, 6H, Ar), 1.30 (s, 27H, *t*-Bu), 2.33 (t, 2H, *n*-Bu), 1.66 (m, 2H, *n*-Bu), 1.35 (m, 2H, *n*-Bu), 0.91 (t, 3H, *n*-Bu). Anal. Calcd for $C_{44}H_{54}N_2O_4$: C, 78.30; H, 8.06; N, 4.15. Found: C, 78.17; H, 8.00; N, 4.25.

2-$Ar_3CCONHC_6H_4COOH$ (L2H)

To a solution of 2-aminobenzoic acid (279 mg, 2.0 mmol) and triethylamine (0.84 mL, 6.0 mmol) in CH_2Cl_2 (10 mL) was added a solution of Ar_3CCOCl (956 mg, 2.0 mmol) in CH_2Cl_2 (10 mL) at 0 °C. After stirring overnight at room temperature, the solution was concentrated under reduced pressure. The residue was mixed with ethyl acetate, washed with 2% HCl aq. and sat. NaCl aq., successively, and dried over Na_2SO_4. After removal of solvents under reduced pressure, the residual powder was recrystallized from CH_2Cl_2/*n*-hexane to afford colorless needles. Yield: 229 g (19.7%). ^{1}H NMR (500 MHz, $CDCl_3$): δ10.64 (s, 1H ,NH), 8.91(dd, 1H, Ar), 8.00 (dd, 1H, Ar), 7.58 (m, 1H, Ar), 7.28 (d, 6H, Ar), 7.20 (d, 6H, Ar), 7.08 (m, 1H, Ar), 1.28 (s, 27H, *t*-Bu). Anal. Calcd for $C_{39}H_{45}NO_3$: C, 81.32; H, 7.88; N, 2.43. Found: C, 81.12; H, 7.79; N, 2.43.

$(NMe_4)[O_2C\text{-}2\text{-}Ar_3CCONH\text{-}6\text{-}n\text{-}BuCONHC_6H_3]$ ((NMe4)[L1])

To a solution of **L1**H (107 mg, 0.16 mmol) in EtOH (30 mL) was added an aqueous solution of tetramethylammonium

View Article Online
DOI: 10.1039/C5DT00053J
ARTICLE

acetate (55 mM, 3.0 mL, 0.17 mmol) and the solution was evaporated . The residue was dissolved in EtOH and evaporated. This manipulation was repeated several times to remove acetic acid completely. The residue was recrystallized from 1,4-dioxane/*n*-hexane to afford colorless needles. Yield: 111 mg (93%). ^{1}H NMR (500 MHz, $CDCl_3$): δ13.05(s, 1H, NH), 12.97(s, 1H, NH), 8.25 (m, 2H, Ar), 7.49 (d, 1H, Ar), 7.25 (s, 12H, Ar), 2.89 (s, 12H, NMe_4^+), 1.28 (s, 27H, *t*-Bu) , 2.33 (t, 2H, *n*-Bu) , 1.66 (m, 2H, *n*-Bu) , 1.35 (m, 2H, *n*-Bu) , 0.91 (t, 3H, *n*-Bu). Anal. Calcd for $C_{52}H_{73}N_3O_6$ ((NMe_4)[**L1**]·(1,4-dioxane)): C, 74.69; H, 8.80; N, 5.03. Found: C, 74.94; H, 8.31; N, 5.37. The presence of 1,4-dioxane was confirmed quantitatively by ^{1}H NMR spectra (at ~3.7 ppm).

(NMe_4)[O_2C-2-Ar_3CCONHC_6H_4] ((NMe_4)[L2])

This compound was synthesized in the same manner described for (NMe_4)[**L1**]] using **L2**H (189 mg, 0.33 mmol) and tetramethylammonium acetate (43.7 mg, 0.33 mmol) to afford colorless needles. Yield: 176 mg (82%). ^{1}H NMR (500 MHz, $CDCl_3$): δ13.37 (s, 1H ,NH), 8.73(dd, 1H, Ar), 8.06 (dd, 1H, Ar), 7.31(m, 1H, Ar), 7.28(d, 12H, Ar), 7.23 (s, 12H, Ar), 3.12 (s, 12H, NMe_4^+), 1.28 (s, 27H, *t*-Bu). Anal. Calcd for $C_{49}H_{68}N_2O_6$ ((NMe_4)[**L2**]·1.5(1,4-dioxane)): C, 75.35; H, 8.78; N, 3.59. Found: C, 75.29; H, 8.30; N, 4.40. The presence of 1,4-dioxane was confirmed by ^{1}H NMR spectra.

[Mg(O_2C-2-Ar_3CCONH-6-*n*-BuCONHC_6H_3)$_2$(H_2O)$_4$] ($MgL1_2$**)**

The metal complexes described in this paper were synthesized by a similar procedure to the literature.[23] To a solution of **L1**H (56.6 mg, 0.084 mmol) in ethanol (30 mL) was added an aqueous solution of $Mg(OAc)_2$·$4H_2O$ (136 mM, 0.32 mL, 0.044 mmol) at room temperature and the solution was dried in vacuo. The residue was dissolved in ethanol, and the solution was evaporated under reduced pressure. This process was repeated several times to remove acetic acid completely. The residue was recrystallized from 1,4-dioxane/water to afford colorless blocks. Yield: 22.1 mg (36%). Anal. Calcd for $C_{97.2}H_{138}MgN_4O_{19.3}$ ([Mg(**L1**)$_2$(H_2O)$_4$]·2.3(1,4-dioxane)·2.7(H_2O)): C, 68.57; H, 8.21; N, 3.28. Found: C, 68.57; H, 8.12; N, 3.30. When the product was recrystallized from EtOH/*n*-hexane, [Mg(O_2C-2-Ar_3CCONH-6-*n*-BuCONHC_6H_3)$_2$(EtOH)$_4$] (**MgL1$_2$**(EtOH)) was obtained as colorless columns. The coordinated EtOH molecules were easily removed under reduced pressure and replaced by H_2O in air.

[Mg(O_2C-2-Ar_3CCONHC_6H_4)$_2$(H_2O)$_4$] ($MgL2_2$**)**

L2H (371 mg, 0.64 mmol) and $Mg(OAc)_2$·$4H_2O$ (75.6 mg, 0.35 mg) were dissolved in a mixture of ethanol and water at room temperature and the solution was dried in vacuo. The residue was dissolved in ethanol, and the solution was concentrated to dryness under reduced pressure. This process was repeated several times as mentioned above. The residue was recrystallized from 1,4-dioxane/water to give colorless needles. Yield: 458 g (76%). Anal. Calcd for $C_{88.4}H_{119}MgN_2O_{16.3}$ ([Mg(**L2**)$_2$(H_2O)$_4$]·2.6(1,4-dioxane)·1.1(H_2O)): C, 70.73; H, 8.05; N, 1.83. Found: C, 70.76; H, 7.93.; N, 1.84. [Mg(O_2C-2-Ar_3CCONHC_6H_4)$_2$(EtOH)$_4$] (**MgL2$_2$**(EtOH)) was also obtained by the recrystallization from EtOH as colorless blocks. The easy release of the EtOH molecules was also observed as mentioned for **MgL1$_2$**(EtOH).

[Zn(O_2C-2-Ar_3CCONH-6-*n*-BuCONHC_6H_3)$_2$(H_2O)$_4$] ($ZnL1_2$**)**

This compound was synthesized by the same method described for **MgL1$_2$** except for using **L1**H (71.5 mg, 0.11 mmol) and $Zn(OAc)_2$ (14.8 mM, 3.70 mL, 0.055 mmol). Recrystallization from 1,4-dioxane/water afforded colorless needles. Yield: 52.7 mg (65%). Anal. Calcd for $C_{96.8}H_{131}N_4O_{16.3}Zn$ ([Zn(**L1**)$_2$(H_2O)$_4$]·2.2(1,4-dioxane) – 0.1(H_2O)): C, 69.32; H, 7.90; N, 3.34. Found: C, 69.55; H, 7.68; N, 3.49.

[Zn(O_2C-2-Ar_3CCONHC_6H_4)$_2$(H_2O)$_4$] ($ZnL2_2$**)**

This compound was synthesized by the same method described for **MgL2$_2$** except for using **L2**H (226 mg, 0.39 mmol) and $Zn(OAc)_2$ (35.1 mg, 0.19 mmol). Colorless needles were obtained. Yield: 43.0 mg (17%). Anal. Calcd for $C_{82}H_{105}N_2O_{12.3}Zn$ ([Zn(**L2**)$_2$(H_2O)$_4$]·1/2(1,4-dioxane)·(H_2O)): C, 71.34; H, 7.69; N, 2.03. Found: C, 71.05; H, 7.38.; N, 2.08.

[Ca_2(O_2C-2-Ar_3CCONH-6-*n*-BuCONHC_6H_3)$_4$(H_2O)$_5$(1,4-dioxane)] (Ca_2L1_4**)**

To a solution of **L1**H (55.1 mg, 0.082 mmol) in ethanol (30 mL) was added an aqueous solution of $Ca(OAc)_2$·H_2O (62.3 mM, 0.6 mL, 0.037 mmol) at room temperature and the solution was dried under reduced pressure. The residue was treated in the same procedure described for **MgL1$_2$**. Recrystallization from 1,4-dioxane/water afforded colorless blocks. Yield: 32.3 mg (59%). Anal. Calcd for $C_{180}H_{230}Ca_2N_8O_{23}$ ([Ca_2(**L1**)$_4$(H_2O)$_5$(1,4-dioxane)]): C, 73.19; H, 7.85; N, 3.79. Found: C, 73.24; H, 8.01; N, 3.82.

Physical measurements

^{1}H nuclear magnetic spectroscopy (^{1}H NMR) spectra were obtained on a JEOL ECS-400 and ECA-500 spectrometers using $CDCl_3$ or CD_2Cl_2 solution at 30 °C or variable temperatures (30, 0, −30, −60, and −90 °C). ^{31}P NMR spectra were obtained on a JEOL ECA-500 spectrometer in $CDCl_3$ at 30 °C, where 85% H_3PO_4 was used as the external standard. ^{13}C NMR, ^{1}H-^{1}H correlation spectroscopy (COSY), nuclear Overhauser effect (NOE) correlated spectroscopy (NOESY), ^{1}H-^{13}C hetero-nuclear single quantum coherence (HSQC), hetero-nuclear multiple bond connectivity (HMBC) spectra of **L1**H and **L2**H were obtained on a Bruker AVANCE700 spectrometer in $CDCl_3$ at 30 °C.

X-ray structure determination

Each single crystal of **L0**H·3(AcOEt), (NMe_4)[**L1**]·2(H_2O)·1,4-dioxane, **L2**H·1/2(1,4-dioxane), **Ca_2L1_4**·4(1,4-dioxane)·4(H_2O), **MgL1$_2$**(EtOH)·4(EtOH), and **MgL2$_2$**(EtOH)·5(EtOH) was selected carefully and mounted on MicroMount™ 200 μm with Nujol, which was frozen immediately in a stream of cold nitrogen at 200 K. Data

collection was made on a Rigaku RAPID II Imaging Plate area detector with Mo-Kα radiation (0.71075 Å) using MicroMax-007HF microfocus rotating anode X-ray generator and VariMax-Mo optics. The structure was solved by direct methods[29,30] and expanded Fourier techniques using SHELXL-2014/6.[30] Non-hydrogen atoms were refined anisotropically. Some H atoms of amide groups were found in the differential Fourier map, then located there, and their coordinates were refined. The other H atoms were generated by the riding and rotating model in SHELXL-97.[30]

Kinetic analysis for hydrolysis of TNPP

A solution of TNPP (5 mM) and **MLn$_2$** (or **Ca$_2$L1$_4$**, 2.5 mM) in CD_2Cl_2 was heated at 50 °C in a sealed NMR tube and the progress of reaction was monitored by the ^{1}H NMR signals of 4-nitrophenol.

Density Functional Theory (DFT) Calculations

Geometry optimizations were performed using Becke's three parameter hybrid functionals (B3LYP) in Gaussian 09[31] program package using 6-31G(d,p) basis set. Initial models, *mer*-[**MgL1$_3$**]$^-$ and *fac*-[**MgL2$_3$**]$^-$, were constructed by the modifications of the X-ray structures, **MgL1$_2$**, **MgL1$_2$**(EtOH), and **MgL2$_2$**. The structures were roughly optimized using 3-21G* basis set. Introduction of *t*-BuCONH groups to *fac*-[**MgL2$_3$**]$^-$ gave initial model of *fac*-[**MgL1$_3$**]$^-$, which was roughly optimized at 3-21G* level. The optimized structures of *mer*-[**MgL1$_3$**]$^-$ and *fac*-[**MgL1$_3$**]$^-$ were re-optimized by using the higher level basis set described above.

Results and discussion

Synthesis of the ligands

A ligand with two bulky Ar_3CCONH- (Ar = 4-*t*-BuC_6H_4) groups, **L0**H, was synthesized by acylation of 2,6-diaminobenzoic acid, which was freshly prepared from 2,6-di(acetylamino)benzoic acid, as described in the literature[23] (Scheme 1). Low temperature is necessary to prevent decarboxylation of the product. The reaction at 50 °C gave 1,3-$(Ar_3CCONH)_2C_6H_4$ as a byproduct. Unsymmetrically substituted ligand, **L1**H, was synthesized by stepwise acylation. The addition of one equivalent of Ar_3CCOCl afforded the desired 2-Ar_3CCONH-6-$NH_2C_6H_3COOH$ and the undesired disubstituted **L0**H, which was separated out as crystals by careful recrystallization from ethanol and subsequently removed by filtration. The intermediate product was purified with up to ~ 90% purity by repeating the recrystallization procedure mentioned above. The second acylation yielded **L1**H. **L1**H is stable in the solid state but gradually decomposed in chloroform or acidic solution at ambient temperature to give a selectively hydrolyzed product, 2-Ar_3CCONH-6-$NH_2C_6H_3COOH$. Such hydrolysis was also observed for 2,6-(*t*-Bu$CONH)_2C_6H_3COOH$ in chloroform. The doubly NH···O hydrogen-bonded carboxylic acid is very acidic[32] and thus the oxygen atom of the amide group was intra- or intermolecularly protonated and then hydrolyzed by traces of water in the solvents. The reaction was dependent on the polarity of the solvents. Hydrolysis did not occur in dimethyl sulfoxide which weakens the hydrogen bond. The hydrolyzed product, 2-*t*-BuCONH-6-$NH_2C_6H_3COOH$, and singly hydrogen-bonded 2-*t*-Bu$CONHC_6H_4COOH$ were stable in chloroform; therefore, a strong "double" hydrogen bond is essential in nonpolar solvents. **L2**H was prepared by a general procedure. Tetramethylammonium salts of **L1**H and **L2**H, (NMe_4)[**L1**] and (NMe_4)[**L2**], were prepared by the reaction with the corresponding acetate, followed by exhaustive removal of the resulting acetic acid under reduced pressure, as described in the literature.[32] These compounds were fully characterized by X-ray analysis, ^{1}H NMR spectroscopy, and elemental analysis.

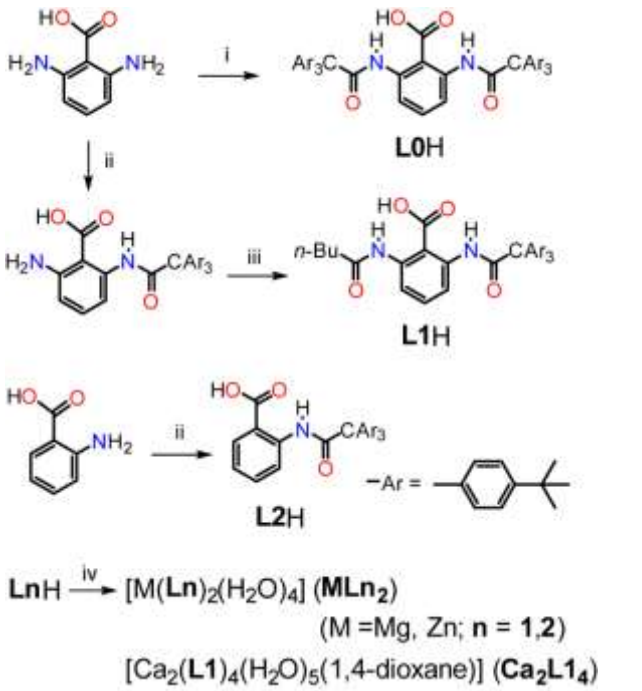

Scheme 1 (i) 2Ar_3CCOCl/NEt_3, CH_2Cl_2, 0 °C. (ii) Ar_3CCOCl/NEt_3, CH_2Cl_2, 0 °C. (iii) *n*-BuCOCl/NEt_3, CH_2Cl_2, -78 °C then 0 °C. (iv) $M(OAc)_2$/EtOH (M = Mg, Zn, Ca) then recryst. from 1,4-dioxane/water.

For **L0**H, (NMe_4)[**L1**], and **L2**H, suitable crystals for X-ray analysis were obtained. The crystallographic parameters and molecular structures are shown in Table S1 and Fig. S1.† The **L0**H molecule was crystallized as a monomeric structure to avoid steric congestion of the bulky substituents. The OH group weakly interacted with ethyl acetate as the crystallization solvent. On the other hand, **L2**H was found as a dimeric structure in the crystal. Such dimerization is quite common and well-known for general carboxylic acids in the solid state or in nonpolar solvents. The tetramethylammonium cation of (NMe_4)[**L1**] is present close to the carboxy group and water of crystallization, demonstrating the presence of intermolecular CH···O hydrogen bonds. In any case, the amide NH group is oriented towards the carboxy group, which strongly suggests the presence of an intramolecular NH···O hydrogen bond.

View Article Online
DOI: 10.1039/C5DT00053J
Journal Name ARTICLE

The ^{1}H NMR spectra of **Ln**H (**n** = **0**–**2**) and (NMe_4)[**Ln**] (**n** = **1**, **2**) in $CDCl_3$ are shown in Fig. S2.† The signals were fully assigned by their correlations using two-dimensional NMR techniques. The downfield shifted signals of NH for (NMe_4)[**L1**] (at 13.04 and 12.64 ppm) and for (NMe_4)[**L2**] (at 13.37 ppm) suggest the presence of strong NH···O hydrogen bonds, as reported previously.[32] The NH signal of **L2**H at 10.55 ppm, further downfield than that of **L0**H at 9.51 ppm, also suggests the presence of a stronger hydrogen bond, which was probably caused by the dimeric structure of **L2**H in $CDCl_3$, similar to that in the crystal mentioned above. The intermolecular OH···O hydrogen bonds increase the electron density on the oxygen atom or the basicity, resulting in a stronger hydrogen bond.

Synthesis of magnesium, zinc, and calcium complexes

The metal carboxylate complexes were synthesized by a ligand-exchange reaction between metal acetate and the corresponding carboxylic acid, followed by exhaustive removal of free acetic acid (Scheme 1), as reported previously.[23] Recrystallization from a hydrous solvent, 1,4-dioxane/water, gave the desired mononuclear complexes [M(**Ln**)$_2$(H_2O)$_4$] (**MLn$_2$**) (M = Mg, Zn; **n** = **1**, **2**). However, the calcium complex was isolated as a crystalline dimeric structure [Ca_2(**L1**)$_4$(H_2O)$_5$(1,4-dioxane)] (**Ca$_2$L1$_4$**) (Chart 1). The reaction between Ca(OAc)$_2$ and **L2**H gave a gel-like product with poor solubility, which could not be characterized. When **MgLn$_2$** (**n** = **1**,**2**) was recrystallized from ethanol under anhydrous conditions, [M(**Ln**)$_2$($EtOH$)$_4$] (**MLn$_2$**($EtOH$)) was obtained as crystals. The coordinated ethanol molecules were easily removed under reduced pressure and were replaced by water molecules in air.

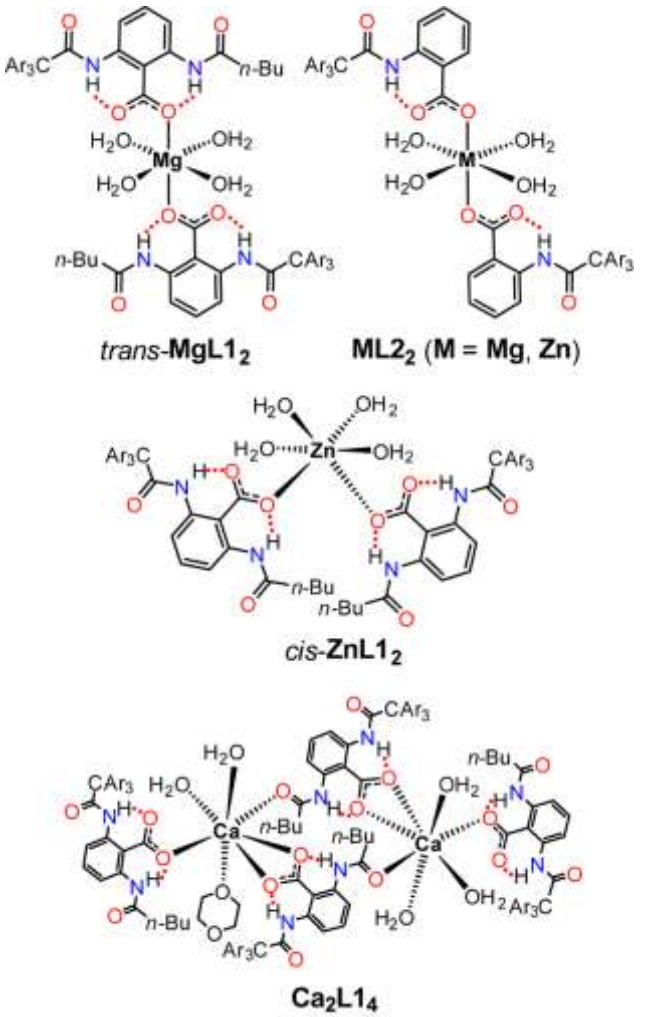

Chart 1 Metal complexes containing NH···O hydrogen bonds.

In the case of **L0**H, similar trials were unsuccessful; therefore, the starting material was changed to the more basic Mg(OCH_3)$_2$. The ^{1}H NMR spectra indicated some perturbations in the presence of metal ions. The aromatic proton signals of the C_6H_3 moiety were shifted upfield and became slightly narrower, while the NH signal was clearly sharpened. These results suggest that some interactions are occurring but that direct coordination is probably absent. Therefore, the most plausible structure is [Mg(H_2O)$_6$][**L0**]$_2$. Such an ion pair of a hydrated magnesium cation and anionic ligands was reported previously.[23] The reaction between Ca(OH)$_2$ and **L0**H gave similar results and recrystallization of the crude product gave crystals of starting **L0**H.

Molecular structures of metal carboxylates

The molecular structures of **MLn$_2$** (**M** = **Mg**, **Zn**; **n** = **1**, **2**) and **Ca$_2$L1$_4$** were determined by X-ray analysis. The structures of **MLn$_2$** have already been communicated previously;[27] therefore, the structural details are now described here. The crystallographic data for **Ca$_2$L1$_4$** are listed in Table S1.† The molecular structures are shown in Fig. 1 and 2. Each

carboxylate ligand was coordinated to a metal ion in a stable *syn* (*Z*) conformation.[33] **MgL1$_2$**, **MgL2$_2$**, and **ZnL2$_2$** were crystallized in the typical *trans* configuration found in many magnesium dicarboxylates;[18,23,34,35] however, **ZnL1$_2$** was crystallized in the *cis* configuration. In the previous paper, we described the formation of magnesium carboxylates containing intramolecular NH···O hydrogen bonds and concluded that a doubly NH···O hydrogen-bonded carboxylate is too weak or soft Lewis base to coordinate directly to the magnesium ion in the *trans* configuration and only the *cis*-dicarboxylate was isolated.[23] Based on this logic, *cis*-**ZnL1$_2$** is the normal structure and *trans*-**MgL1$_2$** is thus a surprising result. We describe here the reason why *trans*-**MgL1$_2$** could be isolated, despite the failure of many trials in the previous paper. The previous complexes were sparingly soluble in nonpolar solvents but dissolved in polar solvents. Polar solvents stabilized hydrated or solvated magnesium ions. Such solvated soft cations should weakly interact with doubly hydrogen-bonded carboxylate anions. The coordinated solvent was hardly removed during recrystallization. The present complex is soluble in nonpolar solvents, which indicates that the Mg^{2+}–**L1**$^-$ ion pair is stabilized in nonpolar solvents and the attack of a water molecule on the magnesium ion must be very limited by the hydrophobic surroundings. In the crystal of **MgL1$_2$**, one water molecule is present near the coordinated water to form OH···O hydrogen bonds (Fig. S3†). The water molecule is buried with a perfect fit in the hydrophobic pocket formed from the Ar_3C and *n*-Bu groups (Fig. S4†). The open front side in Fig. S4a† is covered by 1,4-dioxane in the crystal. The surroundings are probably retained in the recrystallization solvent, i.e., a mixture of 1,4-dioxane/water, resulting in a stable *trans*-dicarboxylate configuration in the crystal. Analogous complexes with the coordination of ethanol instead of water, [Mg(O_2C-2-Ar_3CCONH-6-*n*-BuCONHC_6H_3)$_2$(EtOH)$_4$] (**MgL1$_2$**(EtOH)) and [Mg(O_2C-2-Ar_3CCONHC_6H_4)$_2$(EtOH)$_4$] (**MgL2$_2$**(EtOH)), were crystallized as *cis*-**MgL1$_2$**(EtOH) and *trans*-**MgL2$_2$**(EtOH) structures (Fig. 3). These results suggest that the selection of *trans* or *cis* is unclear and depends on the packing in the crystal. As described below, a fast *trans*-*cis* isomerization should occur in solution.

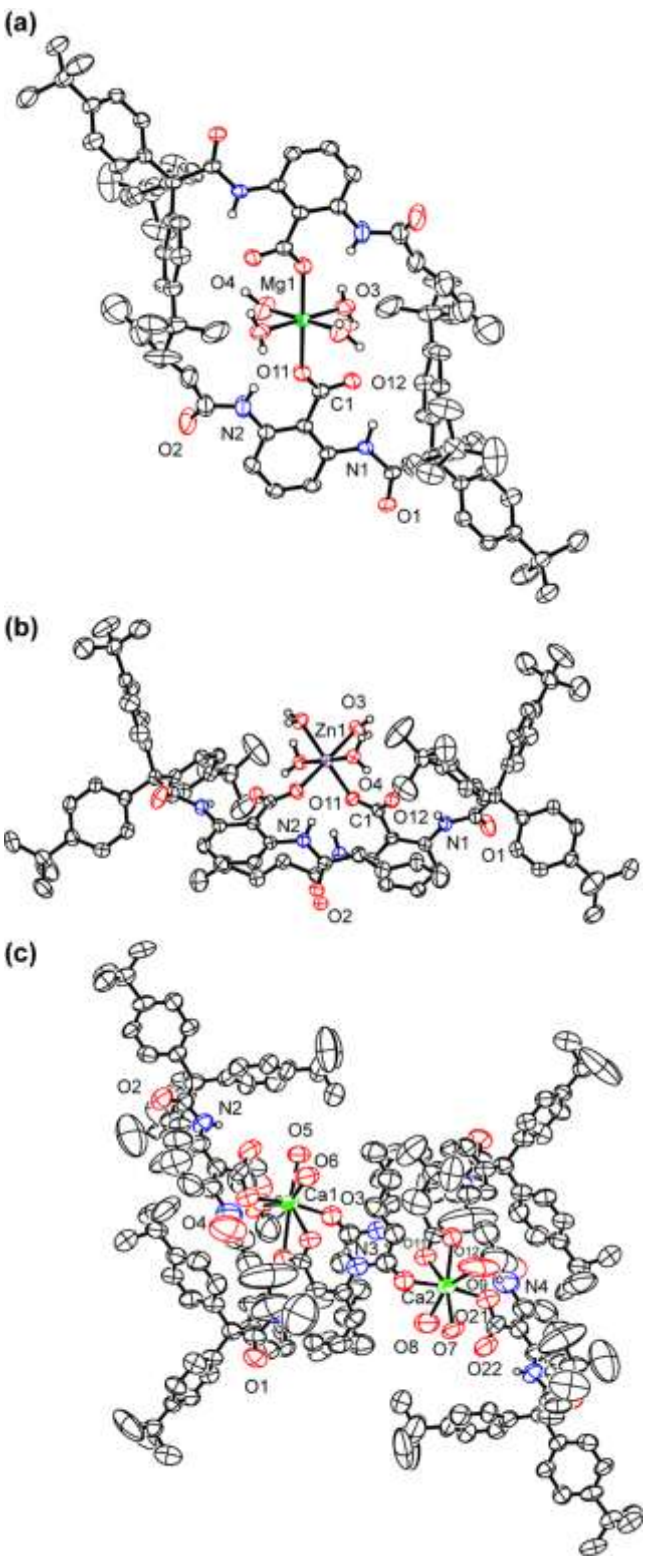

Fig. 1 Molecular structures of (a) *trans*-**MgL1$_2$**, (b) *cis*-**ZnL1$_2$**, and (c) **Ca$_2$L1$_4$**.

View Article Online
DOI: 10.1039/C5DT00053J

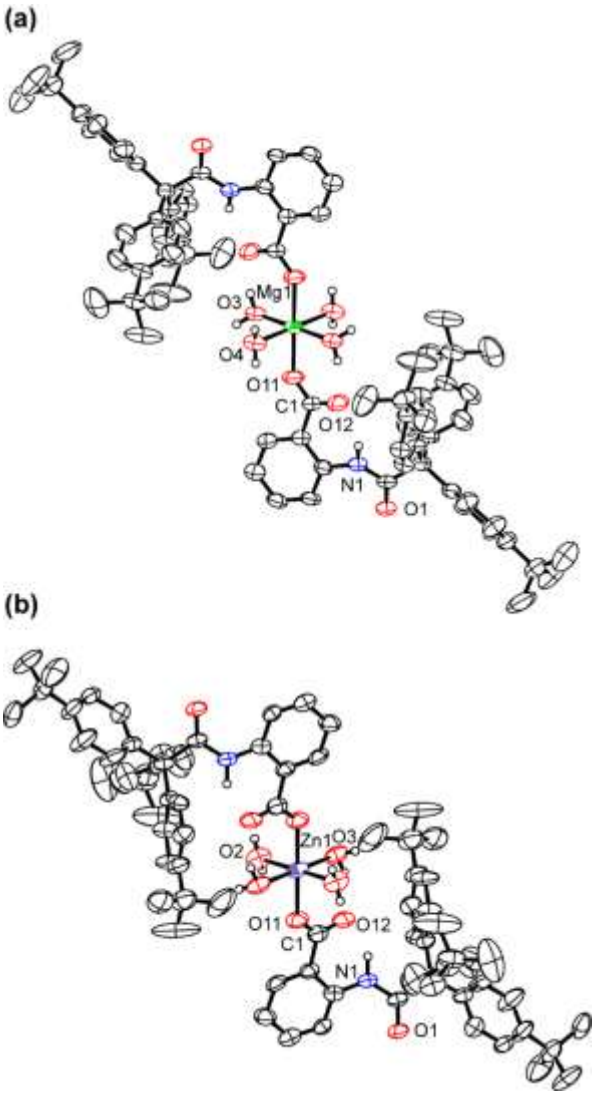

Fig. 2 Molecular structures of (a) **MgL2**$_2$ and (b) **ZnL2**$_2$.

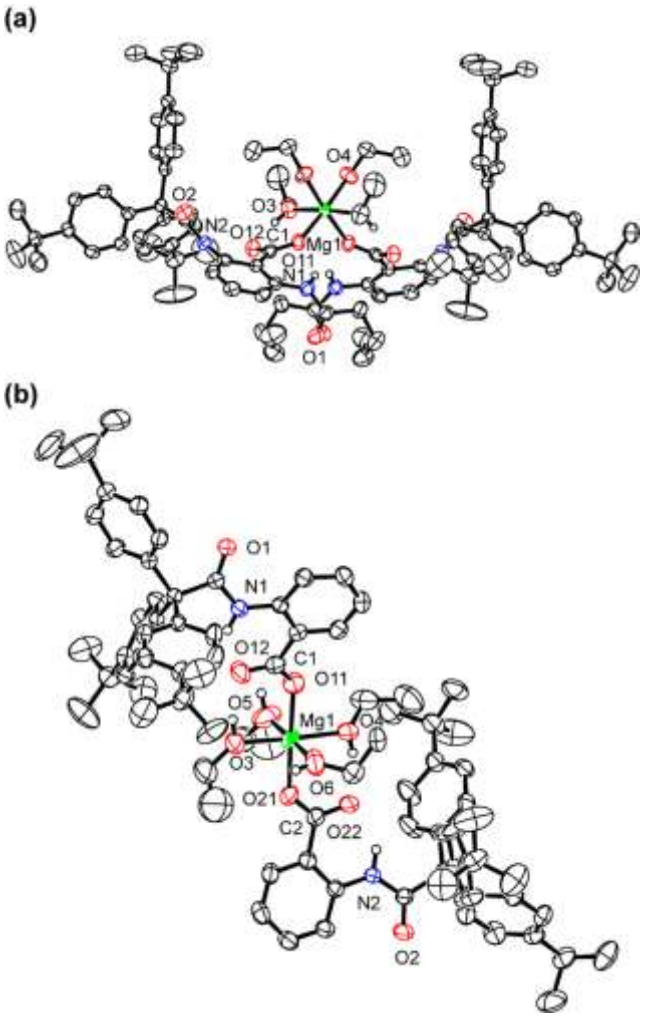

Fig. 3 Molecular structures of (a) **MgL1**$_2$(EtOH) and (b) **MgL2**$_2$(EtOH).

Calcium carboxylates generally prefer bridging or polymeric structures. We previously reported a neutral dimeric calcium complex using a chelate ligand with intramolecular NH···O hydrogen bonds.[36] Because the reaction of $Ca(OAc)_2$ with **L2**H gave a sparingly soluble gel-like complex, the product most likely has polymeric structure. The sufficient bulkiness of **L1** prevented the formation of the polymeric structure to afford dimeric **Ca$_2$L1$_4$** (Chart1, Fig. 1c). The molecule was crystallized in a centrosymmetric space group and a crystallographic inversion center is present at the center of the dinuclear structure. Two calcium atoms were found in close proximity crystallographically; therefore, the structure was solved as an unsymmetrical dimer, assuming that two equivalent disordered parts are present with a half occupancy. The molecule did not contain any bridging carboxylate unit and each calcium site had monomeric, seven-coordinate geometry comprised of chelate and monodentate carboxylates, an amide carbonyl, and three solvent molecules (three water or one 1,4-dioxane and two water molecules). Two Ca–O distances in the chelate carboxylate ligand are significantly different each other like a monodentate ligand. Although the structure was highly disordered and *R* factors were large, the coordination modes of

the carboxylate ligands were found different from the reported η^2-coordination of the analogous carboxylate ligands with NH···O hydrogen bonds.[36,38] Because the coordination number and geometry were very different from the other structures of **MLn$_2$**, the structural comparisons are limited in a series of **MLn$_2$**.

Selected bond distances of **MLn$_2$** (**M** = **Mg**, **Zn**; **n** = **1**, **2**) are listed in Table 1. Intra- and intermolecular hydrogen bonds are shown in Fig. S3.† The M–O (carboxylate) distances are dependent on the mode of the NH···O hydrogen bond as reported previously.[23,27] The hydrogen bond to the uncoordinated oxygen atom of the carboxylate shortens the M–O bond in **ML2$_2$**, while a double NH···O hydrogen bond elongates the M–O (carboxylate) bond in **ML1$_2$**. The M–OH$_2$ bonds are classified into two types; one forms an intramolecular OH···O=C hydrogen bond with the carboxylate ligand and the other intermolecularly hydrogen bonds with crystalline solvents or an amide carbonyl group. The latter M–OH$_2$ bond clearly indicates the opposite tendency to the M–O (carboxylate) bond; that is, the double NH···O hydrogen bond stabilized the short M−OH$_2$ bond. The mean M–OH$_2$ distances were in the order of **ML1$_2$** < **ML2$_2$**. Similar trends were found for Mg–O (carboxylate) distances of *cis*-**MgL1$_2$**(EtOH) and *trans*-**MgL2$_2$**(EtOH) although the dependency of Mg–O (ethanol) was not so clear (Table S2†).

Table1 Selected bond distances (Å) for **MLn$_2$** (**M** = **Mg**, **Zn**; **n** = **1**,**2**)

	MgL1$_2$	**MgL2$_2$**	**ZnL1$_2$**	**ZnL2$_2$**
M–O11	2.053(2)	2.037(3)	2.069(2)	2.040(3)
M–OH$_2$	2.058(2)	2.113(3)	2.132(2)	2.151(4)
	2.083(2)[a]	2.095(3)[a]	2.101(2)[a]	2.100(5)[a]
mean	2.070	2.104	2.117	2.126
C1–O11	1.266(3)	1.261(4)	1.270(3)	1.281(7)
C1–O12	1.259(3)	1.245(5)	1.247(3)	1.228(8)

[a]Forming intramolecular OH···O=C hydrogen bond.

The small difference in the two C–O bond distances in **MgL1$_2$** indicates a delocalized structure for the carboxylate anion. For example, (NMe_4)[**L1**] exhibits approximately equivalent C–O bonds, 1.245(4) and 1.248(4) Å, while **L2**H has single C1–O11 bond (1.316(3) Å) and double C1=O12 (1.223(3) Å) bond. A similar tendency was also found in **L0**H, C1=O11 (1.245(7) Å) and C1–O12 (1.295(7) Å). Therefore, the difference indicates an anionic character for the carboxylate ligand in the complex. The anionic character is estimated in the order of **ML1$_2$** > **ML2$_2$** and **MgLn$_2$** > **ZnLn$_2$**. The oxygen atom of the anionic carboxylate ligand increases the electron density and should form a stronger NH···O hydrogen bond.

The effect of the hydrogen bonds is dependent on the electron density of the oxygen atom. In the ionic Mg–O (carboxylate) bond, electrons are localized on the oxygen atom as compared with the zinc analogue. In the relatively covalent Zn–O bond, electrons are delocalized between zinc and oxygen atoms. The contribution of the hydrogen bond is probably spread over the atoms, therefore, not so effective.

Solution structures of metal carboxylates in nonpolar solvents

The complexes, **MLn$_2$** and **Ca$_2$L1$_4$**, were readily soluble in nonpolar solvents, such as chloroform, dichloromethane, and toluene. The ^{1}H NMR spectra of these complexes in $CDCl_3$ are shown in Fig. 4 and 5 along with the spectra of **L1**H and **L2**H. Very broad signals were observed for all the metal carboxylates although the original **Ln**H showed sharp signals. As described above, **MgL1$_2$** and **ZnL1$_2$** were crystallized with *trans* and *cis* geometry, respectively; therefore, the similarity between the spectra of these complexes suggests a fast *trans*-*cis* isomerization on the NMR time scale (Fig. 4a, b). These spectra revealed the real averaged solution structure in nonpolar solvents. ^{1}H NMR spectra of **ZnL1$_2$** in CD_2Cl_2 were measured at lower temperatures to depress the isomerization; however, broad peaks were not separated and sharpened (Fig. S5†). On the contrary, peaks became broad and complex at −90 °C, which suggests aggregation through intermolecular interactions. However, direct coordination of the amide carbonyl group to the metal ion hardly occurs because of the steric hindrance of the Ar_3C– group.

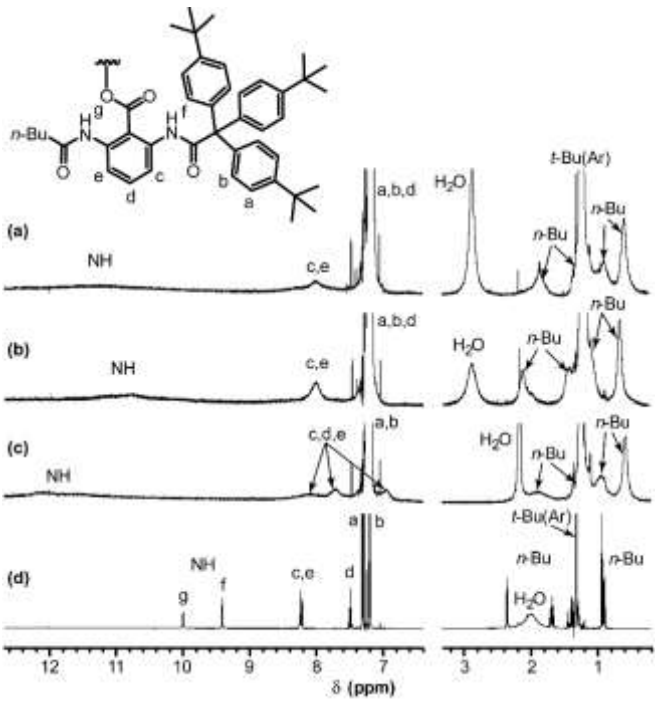

Fig. 4 ^{1}H NMR spectra of (a) **MgL1$_2$**, (b) **ZnL1$_2$**, (c) **Ca$_2$L1$_4$**, and (d) **L1**H in $CDCl_3$.

View Article Online
DOI: 10.1039/C5DT00053J
ARTICLE

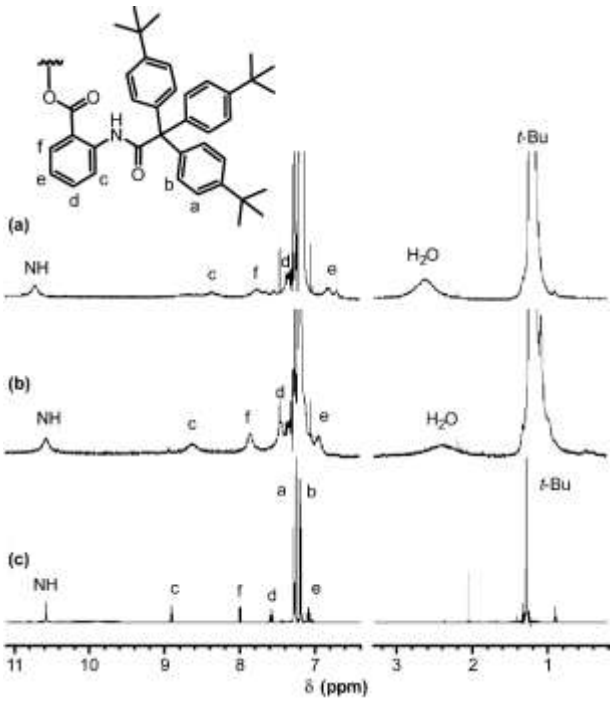

Fig. 5 ^{1}H NMR spectra of (a) **MgL2$_2$**, (b) **ZnL2$_2$**, and (c) **L2**H in $CDCl_3$.

The chemical shifts of the signals for NH and the coordinated water molecules are summarized in Table 2 along with the data for the NH signals of **Ln**H and (NMe_4)[**Ln**]. The downfield shift of the NH signal reflects the strength of the NH···O hydrogen bond. The electron-rich oxygen atom of the anionic carboxylate in (NMe_4)[**L2**] (δ(NH), 13.37 ppm) formed a strong NH···O hydrogen bond. The negative charge in (NMe_4)[**L1**] (13.04 and 12.94 ppm) was shared by two hydrogen bonds, weakening each bond. Free carboxylic acid **L1**H (9.99, 9.40 ppm) formed weak hydrogen bonds, while dimeric **L2**H (10.55 ppm) has polarized carboxy groups, which strengthen the hydrogen bond. The NH signals of **MLn$_2$** were observed within the range of these values (10.58−11.28 ppm) in the order of **ML1$_2$** > **ML2$_2$**, which agreed with the estimated order from the X-ray analysis.

Table 2 ^{1}H NMR signals in $CDCl_3$

	MgL1$_2$	**MgL2$_2$**	**ZnL1$_2$**	**ZnL2$_2$**	**Ca$_2$L1$_4$**
M–OH_2	2.85	2.61	2.86	2.35	2.15
NH	11.28	10.72	11.09, 10.76	10.58	12.09, 11.52
	L1H	**L2**H	(NMe_4)[**L1**]	(NMe_4)[**L2**]	
NH	9.99, 9.40	10.55	13.04, 12.94	13.37	

The signals of the coordinated water molecules of **MLn$_2$** were observed in the range of 2.35−2.86 ppm, while residual free water in $CDCl_3$ is usually detected at ~ 1.5 ppm. Similar spectra were obtained in toluene-d_8. The coordinated water molecules were more downfield-shifted than 2.1 ppm while free water should be at ~ 0.4 ppm.[37] The downfield shifts indicate the acidity of the coordinated water in the order of **ML1$_2$** > **ML2$_2$**, which is consistent with the mean distance or strength of the M–OH_2 bonds in the crystal. The coordinated water molecules of **Ca$_2$L1$_4$** were less acidic.

Preparation of mononuclear anionic magnesium and zinc carboxylates

Previously, we reported an anionic calcium tetrakis(carboxylate) complex, $(NEt_4)_2$[Ca{O_2C-2,6-(*t*-BuCONH)$_2$$C_6H_3$}$_4$], which showed sharp ^{1}H NMR signals in $CDCl_3$.[38] Herein, we attempt to prepare anionic complexes from **MLn$_2$**. Fig. S6† shows the successive addition of (NMe_4)[**L1**] into the solution of **ZnL1$_2$** in $CDCl_3$. The original signals of **ZnL1$_2$** were very broad, as described above. Upon addition of equimolar (NMe_4)[**L1**], the signals clearly became sharp and distinct, which suggested the formation of (NMe_4)[Zn(**L1**)$_3$(H_2O)$_3$] ((NMe_4)[Zn**L1**$_3$]). Another addition did not cause any significant shifts but slightly broadened the signals, indicating a fast (but slow in the NMR time scale) ligand-exchange equilibrium between (NMe_4)[Zn**L1**$_3$] and excess **L1**$^-$. After further addition, the signals of excess (NMe_4)[**L1**] were observed. Because another signal was not detected during the reaction, it can be concluded that (NMe_4)[Zn(**L1**)$_3$] is the most stable structure under these conditions. These results are consistent with the theoretical prediction for water-substitution reactions of magnesium carboxylates in a medium with a low dielectric constant.[12] In a similar manner, analogous complexes (NMe_4)[**MLn$_3$**] (**M** = **Mg**, **Zn**; **n** = **1**, **2**) were prepared. The ^{1}H NMR spectra of these complexes in $CDCl_3$ are shown in Fig. 6. All signals were reasonably assigned. The downfield shifted signals of H_2O indicated that the coordinated water molecules remained. The signals of NMe_4^+ at relatively high field suggested a decreased interionic interaction with a soft [**MLn$_3$**]$^-$ anion, instead of a hard carboxylate (**Ln**$^-$) anion and/or a shielding effect by the spatially neighboring aromatic rings in the hydrophobic media. The signals of (NMe_4)[Zn(**L1**)$_3$] did not split at low temperatures even at −90 °C (Fig. S7).† The signals, including those of the solvents, were broader at −90 °C due to the limitations of taking the measurements in CD_2Cl_2 (close to the melting point). The presence of a single set of the ligands suggests that the three ligands are equivalent; therefore, facial coordination is the most plausible. Two isomers, *fac*- and *mer*-[**ML$_3$**]$^-$, are represented in Chart 2. Possible structures are very limited by the substituent groups. To avoid steric congestion, the very bulky Ar_3C group should be external; that is, near to the uncoordinated carbonyl group.

View Article Online
DOI: 10.1039/C5DT00053J

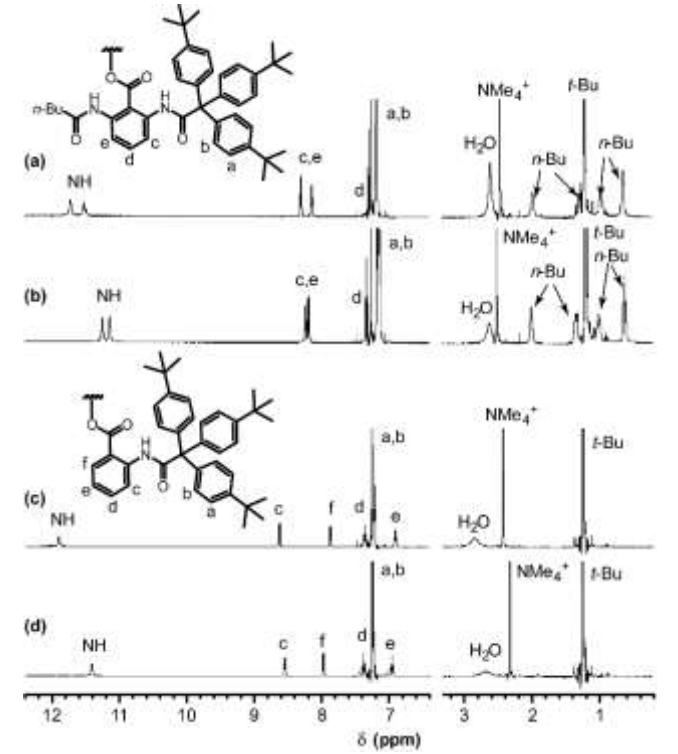

Fig. 6 ^{1}H NMR spectra of (a) $\mathbf{MgL1_2}$ + (NMe_4)[**L1**] ((NMe_4)[$\mathbf{MgL1_3}$]), (b) $\mathbf{ZnL1_2}$ + (NMe_4)[**L1**] ((NMe_4)[$\mathbf{ZnL1_3}$]), (c) $\mathbf{MgL2_2}$ + (NMe_4)[**L2**] ((NMe_4)[$\mathbf{MgL2_3}$]), and (d) $\mathbf{ZnL2_2}$ + (NMe_4)[**L2**] ((NMe_4)[$\mathbf{ZnL2_3}$]) in $CDCl_3$ at 30 °C.

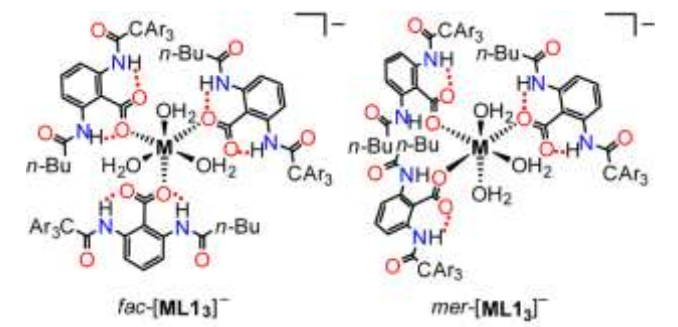

Chart 2 Possible structures of $[ML1_3]^-$ (M = Mg, Zn).

Based on the X-ray structures of $\mathbf{MgLn_2}$, reasonable models were constructed and geometrically optimized using DFT calculations at the B3LYP/6-31G(d,p) level. The optimized structures for two isomers are shown in Fig. S8.† The converged total energy of *fac*-$[\mathbf{MgL1_3}]^-$, with an approximately three-fold rotational symmetry, was lower than that of *mer*-$[\mathbf{MgL1_3}]^-$ by ~ 15 kcal mol^{-1}. In *fac*-$[\mathbf{MgL1_3}]^-$, three Ar_3C groups adequately cover the facial $Mg(H_2O)_3$ site to prevent another coordination and each coordinated water molecule forms an intramolecular OH···O=C hydrogen bond with the uncoordinated oxygen atom of a neighboring carboxy group. A trial to isolate (NMe_4)[$\mathbf{MLn_3}$] by recrystallization failed due to the undesired (NMe_4)[**Ln**] crystallizing first. Such dissociation should occur in solution as described below.

Hydrolysis of TNPP by metal carboxylates in nonpolar solvents

The hydrolytic activities of the complexes were evaluated by stoichiometric reactions with tris(4-nitrophenyl) phosphate (TNPP) in dichloromethane, as communicated previously.[27] A solution of TNPP (5 mM) and each metal carboxylate ($[M^{2+}]$ = 5 mM) in dichlorometane-d_2 afforded a hydrolyzed product, 4-nitrophenol (NP), which was monitored by ^{1}H NMR spectral measurements. The yield of NP was plotted against time for each complex (Fig. 7). Interestingly, naturally occurring magnesium carboxylates were governed by the mode of the NH···O hydrogen bond, while zinc carboxylates were not so affected by the hydrogen bond. Moreover, the biologically inactive calcium carboxylate showed low activity, although it has a unique dimeric structure. The reaction rates were in the order of $\mathbf{ML2_2}$ > $\mathbf{ML1_2}$, which agreed with the strength of the M–O (carboxylate) bond. The order of the initial reaction rates for the three metal ions was $\mathbf{ZnL1_2}$ > $\mathbf{MgL1_2}$ > $\mathbf{CaL1_2}$, which is in agreement with the acidity of the hydrated metal ions. The reported pK_a values of hydrated Zn^{2+}, Mg^{2+}, and Ca^{2+} ions are 9.0, 11.4, and 12.9, respectively.[39] Anionic complex, (NMe_4)[$\mathbf{MgL2_3}$], showed high hydrolytic activity caused by basic free $\mathbf{L2}^-$ anion generated by the dissociation of the ligand; therefore, we could not evaluate the true activity of the anionic complex.

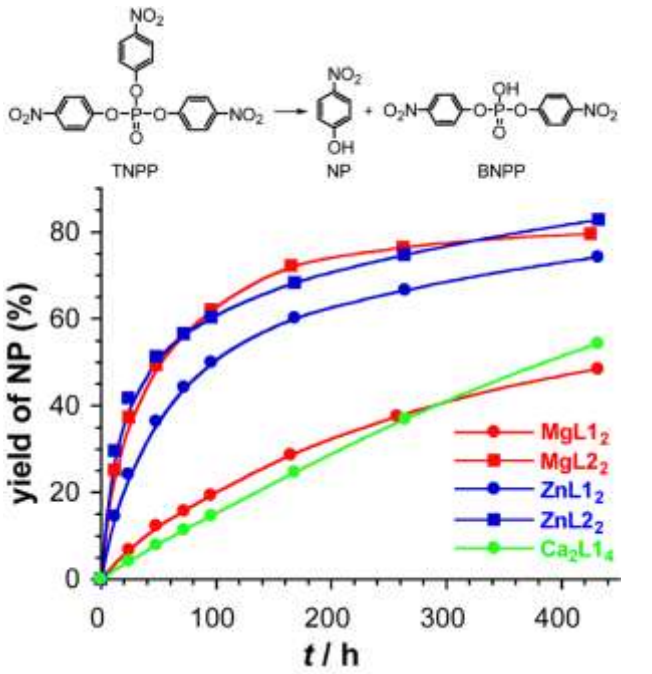

Fig. 7 Time course for the hydrolysis of TNPP by $\mathbf{MLn_2}$ (**M** = **Mg**, **Zn**; **n** = **1**, **2**) or $\mathbf{Ca_2L1_4}$ in CD_2Cl_2 at 50 °C monitored by ^{1}H NMR spectroscopy.

Contributions of NH···O hydrogen bonds

The contributions of NH···O hydrogen bonds are illustrated in Fig. 8. The direct hydrogen bond to the coordinated oxygen atom of the carboxy group elongates the M–O (carboxylate) bond and shortens the M–OH_2 bonds. On the other hand, the hydrogen bond to the uncoordinated oxygen atom has the opposite effect. The strong M–OH_2 bond resulted in a relatively

View Article Online
DOI: 10.1039/C5DT00053J
ARTICLE

high acidity of the coordinated water, which was evaluated by the ^{1}H NMR spectra. The hydrolytic activities are in the same order of the strength of the M–O (carboxylate) bonds for the same metal ion, which suggests that the basicity of the OH^- group, rather than the acidity of OH_2 group, is the essential factor for achieving high reactivity.

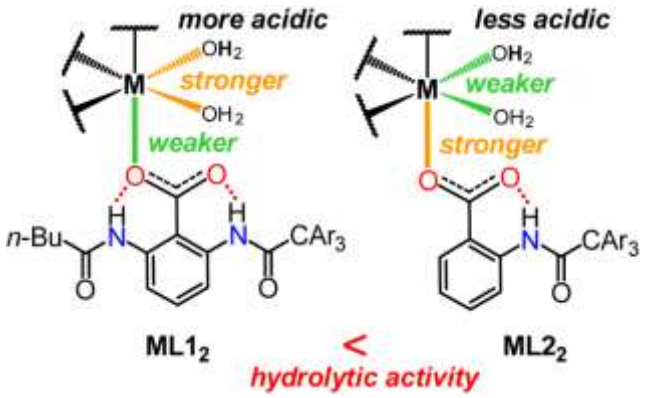

Fig. 8 Contributions of the intramolecular NH···O hydrogen bonds to M–O bonds, acidity of the coordinated water, and hydrolytic activity of phosphoric ester.

Reaction mechanism of the hydrolysis

In the previous paper, we described a proposed mechanism for the hydrolysis in both inner-sphere and outer-sphere pathways.[27] To confirm the interaction between **ML2$_2$** and TNPP in solution, the ^{1}H NMR spectra of **ZnL2$_2$** in the presence and absence of TNPP were measured. The signals of the ligand became slightly sharp with negligible shifts. The signals of TNPP were not affected by **ZnL2$_2$** in $CDCl_3$. However, the signal of the coordinated water molecule was shifted upfield by 0.32 ppm, suggesting the presence of intermolecular interactions. The ^{31}P NMR spectrum of TNPP was negligibly shifted (−0.004 ppm) by the addition of **ZnL2$_2$**, showing little direct bonding between the zinc center and TNPP. Because the amount of the intermediate is probably small, an estimation from NMR spectroscopies is difficult, but the outer-sphere mechanism is the most plausible. An outer-sphere mechanism is sterically favourable in the *trans* configuration, but an inner-sphere mechanism is acceptable in the *cis* configuration.

In the case of **MgL2$_2$**, the dependency on the concentration of the substrate was examined. When the concentration of TNPP was decreased from 5.0 mM to 2.5 mM, the yield of the product after 24 h became approximately half (0.54). However, a 10-fold increase of TNPP (50 mM) resulted in only 2.8 times the yield. Such saturation of the reaction rate against the concentration of substrate is reminiscent of Michaelis–Menten kinetics, which are usually observed in enzymatic reactions. Assuming this type of reaction, K_M was estimated as ~ 16 mM. Moreover, an interesting fact was found regarding this stoichiometric reaction. In the case of 50 mM TNPP, the final yield exceeded the equimolar quantity and achieved 1.8 times of the initial amount of **MgL2$_2$**, suggesting possible catalytic activity.

Conclusions

Soluble magnesium and zinc carboxylates containing intramolecular NH···O hydrogen bonds in nonpolar solvents, e.g. toluene, dichloromethane, and chloroform, were synthesized and their structures were determined. These complexes were mononuclear $[M(\mathbf{Ln})_2(H_2O)_4]$ (M = Mg, Zn; **n** = **1**, **2**) and crystallized in the *trans* or *cis* configuration, although the analogous calcium complex had a dinuclear structure. The M–O (carboxylate) and M–OH_2 distances were regulated by the NH···O hydrogen bonds, depending on the mode, as reported previously.[23] The ^{1}H NMR signals were very broad in nonpolar solvents and suggested a fast *trans*-*cis* isomerization on the NMR timescale. The NMR spectroscopic measurements revealed the acidity of the coordinated water in solution. Equimolar addition of $\mathbf{Ln}^-$ ions sharpened the broad signals clearly, indicating the formation of a unique tris(carboxylate) complex, *fac*-$[\mathbf{MLn_3}]^-$.

Acknowledgements

This work was supported by JSPS KAKENHI (Grant No. 26410072).

Notes and references

Department of Macromolecular Science, Graduate School of Science, Osaka University, Toyonaka, Osaka 560-0043, Japan.
E-mail: tokamura@chem.sci.osaka-u.ac.jp; Fax: +81 6 6850 5474; Tel: +81 6 6850 5451

† Electronic Supplementary Information (ESI) available: X-ray crystallographic data for **L0**H, (NMe_4)[**L1**], **L2**H, **Ca$_2$L1$_4$**, **MgL1$_2$**(EtOH), and **MgL2$_2$**(EtOH), molecular structures, ^{1}H NMR spectra, and optimized structures of $[\mathbf{MgL1_3}]^-$. CCDC 1042059—1042064. See DOI: 10.1039/b000000x/

1. H. Sigel and A. Sigel, eds., *Compendium on magnesium and its role in biology, nutrition and physiology*, Marcel Dekker, New York, 1990, vol. 26.
2. J. A. Cowan, *Chem. Rev.*, 1998, **98**, 1067-1087.
3. J. H. G. Lebbink, A. Fish, A. Reumer, G. Natrajan, H. H. K. Winterwerp and T. K. Sixma, *J. Biol. Chem.*, 2010, **285**, 13131-13141.
4. D. Kostrewa and F. K. Winkler, *Biochemistry*, 1995, **34**, 683-696.
5. Y. Goldgur, F. Dyna, A. B. Hickman, T. M. Jenkins and R. Graigie, *Proc. Natl. Acad. Sci. U. S. A.*, 1998, **95**, 9150-9154.
6. P. Yuan, M. Bartlam, Z. Lou, S. Chen, J. Zhou, X. He, Z. Lv, R. Ge, X. Li, T. Deng, E. Fodor, Z. Rao and Y. Liu, *Nature*, 2009, **458**, 909-913.
7. G. Bujacz, M. Jaskólski, J. Alexandratos, A. Wlodawer, G. Merkel, R. A. Katz and A. M. Skalka, *Structure*, 1996, **4**, 89-96.
8. C. B. Black, H.-W. Huang and J. A. Cowan, *Coord. Chem. Rev.*, 1994, **135/136**, 165-202.
9. J. A. Cowan, *BioMetals*, 2002, **15**, 225-235.
10. C. B. Black and J. A. Cowan, *J. Am. Chem. Soc.*, 1994, **116**, 1174-1178.

View Article Online
DOI: 10.1039/C5DT00053J

11. M. Fothergill, M. F. Goodman, J. Petruska and A. Warshel, *J. Am. Chem. Soc.*, 1995, **117**, 11619-11627.
12. T. Dudev, J. A. Cowan and C. Lim, *J. Am. Chem. Soc.*, 1999, **121**, 7665-7673.
13. T. Dudev and C. Lim, *Acc. Chem. Res.*, 2007, **40**, 85-93.
14. M. Klähn, E. Rosta and A. Warshel, *J. Am. Chem. Soc.*, 2006, **128**, 15310-15323.
15. A. K. Katz, J. P. Glusker, G. D. Markham and C. W. Bock, *J. Phys. Chem. B*, 1998, **102**, 6342-6350.
16. M.-H. Ho, M. D. VIvo, M. D. Peraro and M. L. Klein, *J. Am. Chem. Soc.*, 2010, **132**, 13702-13712.
17. M. D. Vivo, B. Ensing and M. L. Klein, *J. Am. Chem. Soc.*, 2005, **127**, 11226-11227.
18. J.-B. Arlin, A. J. Florence, A. Johnston, A. R. Kennedy, G. J. Miller and K. Patterson, *Cryst. Growth Des.*, 2011, **11**, 1318-1327.
19. S. R. Drake, K. D. Sanderson, M. B. Hursthouse and K. M. A. Malik, *Inorg. Chem.*, 1993, **1993**, 1041-1044.
20. J. W. Yun, T. Tanase and S. J. Lippard, *Inorg. Chem.*, 1996, **35**, 7590-7600.
21. C. S. Babu and C. Lim, *J. Am. Chem. Soc.*, 2010, **132**, 6290-6291.
22. C. S. Babu, T. Dudev and C. Lim, *J. Am. Chem. Soc.*, 2013, **135**, 6541-6548.
23. T. Okamura and J. Nakagawa, *Inorg. Chem.*, 2013, **52**, 10812-10824.
24. T. Okamura, Y. Ushijima, Y. Omi and K. Onitsuka, *Inorg. Chem.*, 2013, **52**, 381-394.
25. Y. Hasenaka, T. Okamura, M. Tatsumi, N. Inazumi and K. Onitsuka, *Dalton Trans.*, 2014, **43**, 15491-1550.
26. T. Dudev and C. Lim, *Chem. Rev.*, 2014, **114**, 538-556.
27. T. Okamura, R. Furuya and K. Onitsuka, *J. Am. Chem. Soc.*, 2014, **136**, 14639-14641.
28. Y. Yamada, N. Ueyama, T. Okamura, W. Mori and A. Nakamura, *Inorg. Chim. Acta*, 1998, **275-276**, 43-51.
29. A. Altomare, M. C. Burla, M. Camalli, M. Cascarano, C. Giacovazzo, A. Guagliardi and G. Polidori, *J. Appl. Crystallogr.*, 1994, **27**, 435.
30. G. M. Sheldrick, *Acta Cryst.*, 2008, **A64**, 112-122.
31. M. J. Frisch, G. W. Trucks, H. B. Schlegel, G. E. Scuseria, M. A. Robb, J. R. Cheeseman, G. Scalmani, V. Barone, B. Mennucci, G. A. Petersson, H. Nakatsuji, M. Caricato, X. Li, H. P. Hratchian, A. F. Izmaylov, J. Bloino, G. Zheng, J. L. Sonnenberg, M. Hada, M. Ehara, K. Toyota, R. Fukuda, J. Hasegawa, M. Ishida, T. Nakajima, Y. Honda, O. Kitao, H. Nakai, T. Vreven, J. A. Montgomery, Jr., J. E. Peralta, F. Ogliaro, M. Bearpark, J. J. Heyd, E. Brothers, K. N. Kudin, V. N. Staroverov, T. Keith, R. Kobayashi, J. Normand, K. Raghavachari, A. Rendell, J. C. Burant, S. S. Iyengar, J. Tomasi, M. Cossi, N. Rega, J. M. Millam, M. Klene, J. E. Knox, J. B. Cross, V. Bakken, C. Adamo, J. Jaramillo, R. Gomperts, R. E. Stratmann, O. Yazyev, A. J. Austin, R. Cammi, C. Pomelli, J. W. Ochterski, R. L. Martin, K. Morokuma, V. G. Zakrzewski, G. A. Voth, P. Salvador, J. J. Dannenberg, S. Dapprich, A. D. Daniels, O. Farkas, J. B. Foresman, J. V. Ortiz, J. Cioslowski and D. J. Fox, *Gaussian 09 (Revision C.01)*, (2010) Gaussian, Inc., Wallingford CT.
32. A. Onoda, Y. Yamada, J. Takeda, Y. Nakayama, T. Okamura, M. Doi, H. Yamamoto and N. Ueyama, *Bull. Chem. Soc. Jpn.*, 2004, **77**, 321-329.
33. C. J. Carrell, H. L. Carrell, J. Erlebacher and J. P. Glusker, *J. Am. Chem. Soc.*, 1988, **110**, 8651-8656.
34. D. E. Irish, J. Semmler, N. J. Taylor and G. E. Toogood, *Acta Crystallogr., Sect. C: Cryst. Struct. Commun.*, 1991, **47**, 2322-2324.
35. B. K. Dey, A. Karmakar and J. B. Baruash, *J. Mol. Cat. A: Chem.*, 2009, **303**, 137-140.
36. N. Ueyama, J. Takeda, Y. Yamada, A. Onoda, T. Okamura and A. Nakamura, *Inorg. Chem.*, 1999, **38**, 475-478.
37. G. R. Fulmer, A. J. M. Miller, N. H. Sherden, H. E. Gottlieb, A. Nudelman, B. M. Stoltz, J. E. Bercaw and K. I. Goldberg, *Organometallics*, 2010, **29**, 2176-2179.
38. A. Onoda, Y. Yamada, Y. Nakayama, K. Takahashi, H. Adachi, T. Okamura, A. Nakamura, H. Yamamoto, N. Ueyama, D. Vyprachticky and Y. Okamoto, *Inorg. Chem.*, 2004, **43**, 4447-4455.
39. T. Pan, D. M. Long and O. C. Uhlenbeck, in *The RNA World*, eds. R. F. Gesteland and J. F. Atkins, Cold Spring Harbor Laboratory Press, Cold Spring Harbor, New York, 1993, pp. 271-302.
40. C. B. Black and J. A. Cowan, *Eur. J. Biochem.*, 1997, **243**, 684-689.

View Article Online
DOI: 10.1039/C5DT00053J

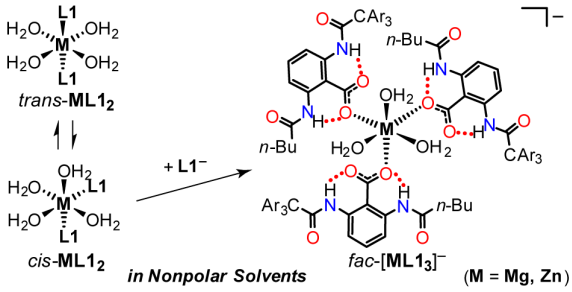

Magnesium and zinc carboxylates containing intramolecular NH···O hydrogen bonds showed a fast *trans-cis* isomerization in nonpolar solvents and were converted into anionic tris(carboxylate)s by the addition of equimolar ligand.